Model Predictive Control of Spacecraft Formations with Sensing Noise

Louis Breger and Jonathan How
Aerospace Controls Laboratory
MIT Department of Aeronautics and Astronautics
{lbreger, jhow}@mit.edu

Arthur Richards
Department of Aerospace Engineering
arthur.richards@bristol.ac.uk

***Abstract*— This paper extends previous analysis on the impact of sensing noise upon the performance of model predictive control of formation flying spacecraft. We present a method of predicting the performance of the closed-loop system in the presence of sensing noise and demonstrate its effectiveness for the spacecraft relative motion problem. Its performance predictions are verified through simulation and used to analyze the effects of formation flying mission parameter trades without recourse to extensive numerical simulation. Ideal values for several model predictive control parameters are identified.**

Keywords: Spacecraft Formation Flying, Model Predictive Control, Sensor Noise

I. INTRODUCTION

Formation flying for spacecraft is an attractive technology for several forthcoming missions [1], [2]. This approach has significant advantages over a single spacecraft, such as greater science return due to longer observation baselines, and increased flexibility. The problem of controlling spacecraft in formation is extremely challenging, requiring precise control without excessive fuel use. Recent studies [8], [14] have shown that sensing uncertainty is a significant driver of control design. This paper makes contributions to this field by applying a technique for analytically predicting the control effort of a predictive control scheme in the presence of sensing uncertainty to the spacecraft formation flying problem.

The model predictive control (MPC) approach is well-suited to formation control because it emphasizes planning rather than immediate feedback, directly accounts for realistic mission constraints, and explicitly optimizes fuel usage [7]. The planning aspect of model predictive control is effective when system dynamics are well known, as is the case for space vehicles. Constraints on spacecraft usually include restrictions on when and how much thruster firing can occur and how much state error can be tolerated; all three types of constraints are easily incorporated into an optimization-based planner. The form of MPC used in this work is developed in [10] and uses repeated replanning over a finite horizon to achieve robustness to process noise and sensing noise.

The closed-loop control effort of the robust control scheme in [10] can be predicted analytically under certain conditions, enabling fast trade studies involving performance and controller parameters [15]. For instance, intuition suggests that there might be an optimal setting of the replan rate to minimize fuel use: too slow and errors accumulate causing large deviations and aggressive corrective action; too fast and the control reacts to sensing noise and wastes fuel with high frequency corrections. The performance analysis tool enables a rapid investigation of this trade-off without the need for extensive numerical simulations at many different rate settings. The analysis in Section III identifies the ideal replan rate and also preferable settings for plan length, as well as other key trades in the mission design. The remainder of the paper is devoted to applying the robustly-feasible MPC scheme to the problem of controlling spacecraft relative motion. Hill's equations of relative motion in a circular orbit are used to model a formation flying control problem in which a spacecraft is constrained to remain inside an error box. Some assumptions about the noise source and the error box are made when using the predictive method and validated by simulation. The analytical prediction method is then used to examine a wide range of missions in order to identify trends, sensitivities, and optimal regions in the space of controller parameters, such as error box size, sensor noise, fuel use, replan frequency and the planning horizon length. The validity of these relations is established and their application to designing future spacecraft formation flying missions is demonstrated using relevant parameter ranges. A number of realistic and desirable parameter combinations are identified, indicating the value of future research to extend and refine the analysis tool.

II. ROBUST MPC FOR ESTIMATION UNCERTAINTY

This section reviews robust Model Predictive Control for problems with inaccurate state information [16]. Then the method of [15] is applied to analytically predict the expected control effort of this controller.

A. Problem Statement

The dynamics of the true state are

$$\mathbf{x}(k+1) = \mathbf{A}\mathbf{x}(k) + \mathbf{B}\mathbf{u}(k) \tag{1}$$

and the estimation error is an additive term, applied at each time step

$$\begin{aligned} \hat{\mathbf{x}}(k) &= \mathbf{x}(k) + \mathbf{M}\mathbf{e}(k) && (2)\\ \hat{\mathbf{x}}(k+1) &= \mathbf{x}(k+1) + \mathbf{M}\mathbf{e}(k+1) && (3) \end{aligned}$$

where $\mathbf{M}$ is a matrix of appropriate dimension and the error $\mathbf{e}(k) \in \Re^{N_e}$ is uniformly distributed in a hypercube

$$\mathbf{e}(k) \in \mathcal{B}_\infty(W_a) \tag{4}$$

where W_a is the norm limit of the error. In this work, the error bound W_a is assumed known, however this assumption can be relaxed [17]. Also assume output constraints of the form

$$\mathbf{y}(k) = \mathbf{C}\hat{\mathbf{x}}(k) + \mathbf{D}\mathbf{u}(k) \in \mathcal{Y} \quad \forall k \tag{5}$$

where $\mathcal{Y}$ is a bounded set. Note that this form can capture many common constraints such as actuation limits and error boxes. Also note that the constraint acts upon the *estimated* state, for that is known. Given the assumption of a bounded state uncertainty, this can be readily transformed to and from equivalent constraints on the actual state [15]. Since the feasibility of the optimization depends only on the estimate and not the truth, the form of (5) is appropriate here.

B. Review of Robust MPC with Sensing Noise

For the spacecraft formation flying problem with sensor noise, robust feasibility guarantees that, provided the initial optimization is feasible and the noise is bounded, all subsequent optimizations are feasible and constraints are satisfied, *e.g.* the spacecraft remains inside the specified error box. This guarantee holds despite the plans being based on inaccurate information.

The key to the robust MPC with state error is the transformation, introduced in [6], to an equivalent problem with perfect information. Substituting (2) and (3) into (1) gives the dynamics of the estimate $\hat{\mathbf{x}}$

$$\hat{\mathbf{x}}(k+1) = \mathbf{A}\hat{\mathbf{x}}(k) + \mathbf{B}\mathbf{u}(k) + \mathbf{M}\mathbf{e}(k+1) - \mathbf{A}\mathbf{M}\mathbf{e}(k) \tag{6}$$

The state of this system (*i.e.*, the estimate $\hat{\mathbf{x}}$) is perfectly known and the last two terms constitute an affine disturbance, bounded according to (4), hence the formulation of [10] can be employed to synthesize a robustly feasible MPC scheme. First, assume that the affine disturbance vector can be bounded as follows

$$\hat{\mathbf{w}}(k) = -\mathbf{A}\mathbf{M}\mathbf{e}(k) + \mathbf{M}\mathbf{e}(k+1) \in \hat{\mathcal{W}} \quad \forall k \tag{7}$$

In our case, the set $\hat{\mathcal{W}}$ is polyhedral and of the form $\mathbf{A}\mathbf{x} \leq \mathbf{b}$ and can therefore be generated using a polyhedral mapping routine of the form in [4].

To determine the constraints in the MPC optimization, the designer chooses a nilpotent linear control law $\mathbf{u}(j) = \mathbf{K}_{NP}\mathbf{x}(j)\ \ j \in \{0 \ldots N-1\}$. Define $\mathbf{L}(j)$ as the state transition matrix for the closed-loop system under this control law

$$\begin{aligned} \mathbf{L}(0) &= \mathbf{I} && (8)\\ \mathbf{L}(j+1) &= (\mathbf{A} + \mathbf{B}\mathbf{K}_{NP})\,\mathbf{L}(j) \quad \forall j \in \{0 \ldots N\} && (9) \end{aligned}$$

Then the nilpotency requirement for $\mathbf{K}_{NP}$ implies $\mathbf{L}(N) = \mathbf{0}$. This control is used to determine constraint tightening margins [10] such that every optimization has a candidate feasible solution, for all disturbances obeying (7), combining the solution to the previous optimization and a perturbation using the controller $\mathbf{K}_{NP}$.

Define the MPC problem $\mathsf{P}(\hat{\mathbf{x}}(k))$ optimizing over a horizon of N steps

$$J^*(\hat{\mathbf{x}}(k)) = \min_{\mathbf{u},\mathbf{x},\mathbf{y}} \sum_{j=0}^{N} \ell\left(\mathbf{u}(k+j|k), \mathbf{x}(k+j|k)\right) \tag{10}$$

subject to $\forall j \in \{0 \ldots N\}$

$$\begin{aligned} \mathbf{x}(k+j+1|k) &= \mathbf{A}\mathbf{x}(k+j|k) + \mathbf{B}\mathbf{u}(k+j|k) && (11)\\ \mathbf{y}(k+j|k) &= \mathbf{C}\mathbf{x}(k+j|k) + \mathbf{D}\mathbf{u}(k+j|k) && (12)\\ \mathbf{x}(k|k) &= \hat{\mathbf{x}}(k) && (13)\\ \mathbf{x}(k+N+1|k) &\in \mathcal{X}_F && (14)\\ \mathbf{y}(k+j|k) &\in \mathcal{Y}(j) && (15) \end{aligned}$$

where the double subscript notation $(k+j|k)$ denotes the prediction made at time k of a value at time $k+j$. The constraint sets are chosen according to the recursion

$$\begin{aligned} \mathcal{Y}(0) &= \mathcal{Y} && (16)\\ \mathcal{Y}(j+1) &= \mathcal{Y}(j) \sim (\mathbf{C} + \mathbf{D}\mathbf{K}_{NP})\,\mathbf{L}(j)\hat{\mathcal{W}} && (17)\\ &\qquad \forall j \in \{0 \ldots N\} \end{aligned}$$

where $\sim$ denotes the Pontryagin difference operation [13], defined by

$$\mathcal{X} \sim \mathcal{Y} \stackrel{\triangle}{=} \{\mathbf{z} \mid \mathbf{z} + \mathbf{y} \in \mathcal{X}\ \forall \mathbf{y} \in \mathcal{Y}\} \tag{18}$$

and the matrix mapping of a set is defined such that

$$\mathbf{A}\mathcal{X} \stackrel{\triangle}{=} \{\mathbf{z} \mid \exists \mathbf{x} \in \mathcal{X} : \mathbf{z} = \mathbf{A}\mathbf{x}\} \tag{19}$$

A Matlab toolbox for performing these operations on polyhedral sets is available in [4].

The terminal constraint $\mathcal{X}_F$ is chosen by the user. It must be a control invariant admissible set [5], *i.e.*, there exists a control law $\kappa(\mathbf{x})$ satisfying the following

$$\begin{aligned} &\forall \mathbf{x} \in \mathcal{X}_F \\ \mathbf{A}\mathbf{x} + \mathbf{B}\kappa(\mathbf{x}) &\in \mathcal{X}_F && (20)\\ \mathbf{C}\mathbf{x} + \mathbf{D}\kappa(\mathbf{x}) &\in \mathcal{Y}(N) && (21) \end{aligned}$$

The choice of terminal set is problem-specific. The origin $\mathcal{X}_F = \{\mathbf{0}\}$ is a straightforward choice, and is used in the following section to enable the performance analysis,

but it may be a restrictive choice for some applications. The Invariant Set Toolbox for Matlab [4] includes a routine to calculate the largest control invariant set within a given set of constraints, which is a preferable choice for some applications. It is not necessary to know the control law κ, only to know that a suitable law exists.

Algorithm Robustly Feasible Estimate MPC

1) Form estimate of current state $\hat{\mathbf{x}}(k)$
2) Solve problem $\mathsf{P}(\hat{\mathbf{x}}(k))$
3) Apply control $\mathbf{u}(k) = \mathbf{u}^*(k|k)$ from the optimal sequence
4) Go to Step 1

This formulation guarantees robust feasibility and constraint satisfaction. The proof is presented in [15], [16] and is not reproduced here, for brevity. The core of the method is the constraint tightening embodied in (18), constituting a "margin" for later feedback action. This is chosen such that at each step, the addition of the predetermined, nilpotent policy to the remainder of the previous plan forms a feasible solution to the new optimization, for all possible disturbances in the set $\hat{\mathcal{W}}$. Thus feasibility at time k implies feasibility at time $k+1$ and therefore, by recursion, initial feasibility implies feasibility of all future problems.

C. Performance Prediction with Sensing Noise

This section extends the formulation of [15] for the sensing noise problem. First, it is necessary to introduce some assumptions to enable the analysis.

1) The performance index is a quadratic function of the control input and the state , $\ell(\mathbf{u}, \mathbf{x}) = \mathbf{x}^T\mathbf{Q}\mathbf{x} + \mathbf{u}^T\mathbf{R}\mathbf{u}$ where $\mathbf{Q}$ and $\mathbf{R}$ are positive definite.
2) The terminal constraint is the origin, $\mathcal{X}_F = \{\mathbf{0}\}$ (note that this trivially satisfies the invariancy requirement with $\kappa(\mathbf{x}) = \mathbf{0}$).
3) The estimation error $\mathbf{e}(k)$ is uniformly distributed in a hypercube as described in (4).
4) The constraint set $\mathcal{Y}$ is a polytope defined by N_p inequalities: $\mathcal{Y} = \{\mathbf{y} | \mathbf{p}_n^T\mathbf{y} \leq q_n \forall n \in 1 \dots N_p\}$

Note that although the dynamics (6) include an affine disturbance signal, that signal has significant autocorrelation: its upper half is simply a delayed copy of its lower half. To eliminate this feature, the dynamics are augmented with additional states to capture the delay, resulting in the following system

$$\left[\begin{array}{c} \hat{\mathbf{x}}(k+1) \\ \mathbf{e}(k+1) \end{array}\right] = \left[\begin{array}{c|c} \mathbf{A} & -\mathbf{A}\mathbf{M} \\ \hline \mathbf{0} & \mathbf{0} \end{array}\right] \left[\begin{array}{c} \hat{\mathbf{x}}(k) \\ \mathbf{e}(k) \end{array}\right] + \left[\begin{array}{c} \mathbf{B} \\ \hline \mathbf{0} \end{array}\right] \mathbf{u}(k) + \left[\begin{array}{c} \mathbf{M} \\ \mathbf{I} \end{array}\right] \mathbf{e}(k+1) \quad (22)$$

Note that this system appears unusual as it is driven by a "look-ahead" input $\mathbf{e}(k+1)$. This is permissible in this case as only the statistical properties of the signal $\mathbf{e}(k)$ are assumed known for the performance analysis.

Assume for the moment that the control law is a constant matrix state feedback operating on the known state estimate

$$\mathbf{u}(k) = \mathbf{K}\hat{\mathbf{x}}(k) \quad (23)$$

Then the system (22) becomes the following

$$\left[\begin{array}{c} \hat{\mathbf{x}}(k+1) \\ \mathbf{e}(k+1) \end{array}\right] = \left[\begin{array}{c|c} \mathbf{A}+\mathbf{B}\mathbf{K} & -\mathbf{A}\mathbf{M} \\ \hline \mathbf{0} & \mathbf{0} \end{array}\right] \left[\begin{array}{c} \hat{\mathbf{x}}(k) \\ \mathbf{e}(k) \end{array}\right] + \left[\begin{array}{c} \mathbf{M} \\ \mathbf{I} \end{array}\right] \mathbf{e}(k+1) \quad (24)$$

Further, if the performance metric is the control effort, the following performance output equation can be used

$$\mathbf{u}(k) = \left[\begin{array}{c|c} \mathbf{K} & \mathbf{0} \end{array}\right] \left[\begin{array}{c} \hat{\mathbf{x}}(k) \\ \mathbf{e}(k) \end{array}\right] \quad (25)$$

so the problem of predicting control effort under the action of state uncertainty and a constant feedback (23) is equivalent to predicting the output of the LTI system (24) and (25). Assuming the bounded disturbance can be treated like a Gaussian distribution and using a quadratic performance metric for $\mathbf{u}$, this can be readily done by solving Lyapunov's equation or using power gain methods [12]. Denote the power gain of system (24) and (25) with control $\mathbf{K}$ by $G(\mathbf{K})$. Although the noise signal is uniformly distributed within a hypercube, as opposed to the customary Gaussian, the central limit theorem is invoked to claim that the output signal still has a Gaussian distribution [3]. Experiments have verified this assumption.

The MPC control law is nonlinear, due to the presence of constraints in the optimization. However, the fuel use as a function of estimation error covariance can be approximated by the function shown in Fig. 1, in which the function $f(\bar{N})$ is the predicted fuel use for noise bound $\bar{N}$. The method is presented only briefly here and the reader is directed to [15] for more information. The basis of the approximation is the assumption that the closed-loop system, including the robust MPC, behaves as particular LTI systems in different regimes of noise covariance. At noise levels approaching zero, the constraints are rarely active, and hence the lower asymptote (line OA in the figure) is the performance for the unconstrained LQR controller, with slope $G(\mathbf{K}_{LQR})/\sqrt{3}$ (the factor of $\sqrt{3}$ arises because $\bar{N}$ is the noise bound and not its standard deviation). The point A, or "cut-off point" is the noise level N^C at which the constraints become significant. This is the level at which the 3σ envelope of the outputs $\mathbf{y}(k+j|k)$ from the unconstrained solution using $\mathbf{K}_{LQR}$ intersects the boundaries of the constraint sets $\mathcal{Y}(j)$. Recall from (18) that the constraints tighten as the noise level increases as a greater margin is withheld for robustness. Point B is the "limit of feasibility," beyond which the constraint tightening makes the problem infeasible, *i.e.* $\mathcal{Y}(N) = \emptyset$. Because of the way the margin is devised, at point B, the optimization has only one solution, that is to apply the predetermined nilpotent control law $\mathbf{K}_{NP}$. Hence the performance at this point can also be predicted using the

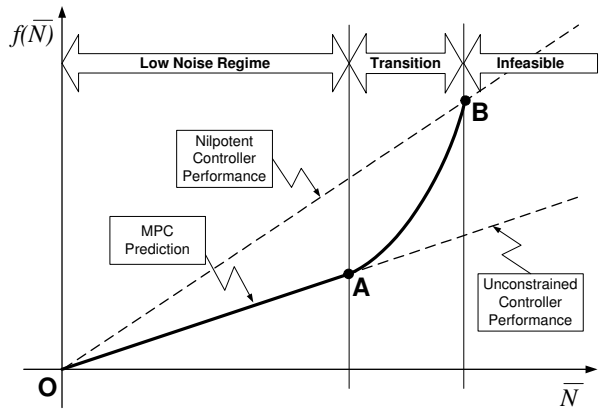

Fig.1: Robust Performance Overview

power gain $G(\mathbf{K}_{NP})$. The nature of the transition region between points A and B is not exactly known and is the subject of on-going research, but it can be approximated by a parabola, tangential to OA at A and passing through B. For brevity, the prediction method presented in this paper assumes that the disturbance bound used to formulate the MPC optimization problem is the same as the actual disturbance. Ref. [17] presents a more full development of the prediction method that accounts for discrepancies between the predicted and the actual disturbances.

III. SPACECRAFT FORMATION FLYING RESULTS

This section describes the application and verification of the analysis method developed in Section II-C to the spacecraft formation flying control problem. The specific application examined is relative motion in a circular orbit using the radial/in-track plane in Hill's equations. The prediction method uses velocity noise sources and a square error box constraint. For the spacecraft formation control problem, the performance is dominated by the effects of the velocity estimation error [14], hence the model can still capture the behavior of the system without incorporating position error.

The system used for analysis will use impulsive velocity changes in both the in-track and radial directions as control inputs. The system is driven by the velocity noises, with $\mathbf{M} = \mathrm{diag}(0, 0, 1, 1)$ and assumes perfect knowledge of the position states. Only the spacecraft states are constrained, so $\mathbf{C} = \mathbf{I}_4$ and $\mathbf{D} = \mathbf{0}_{4\times 2}$. The approximation of dominant velocity noise is valid for a formation using carrier-phase differential GPS [14]. A constant K_{NP} can be found that drives a state in the radial/in-track plane of the Hill's frame to the origin in 4 steps (which restricts the horizon length to $N \geq 4$). This example will use an orbit with frequency $n = 0.001$ (low Earth orbit) and with a discretization $T \approx 314s$ (twenty steps per orbit). The MPC controller is implemented with $N = 5$ predictive steps and a ± 5 meter error box ($Y_{\max} = 5$) is placed around the origin in the in-track direction. The constraint set $\mathcal{Y}$ is given by

$$\begin{bmatrix} I_2 & 0_2 \\ -I_2 & 0_2 \end{bmatrix} \mathbf{y} \leq Y_{\max} \begin{bmatrix} 1 & 1 & 1 & 1 \end{bmatrix}^T \quad \forall\, \mathbf{y} \in \mathcal{Y}$$

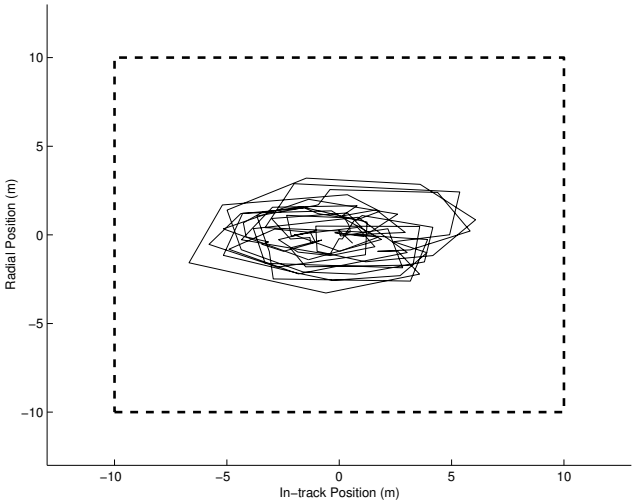

Fig.2: Simulation trajectory using MPC controller (6 orbits shown)

A typical trajectory for spacecraft relative motion using the MPC controller with the system is shown in Figure 2. Although both the radial and in-track positions are constrained in the control formulation, the coupling between the directions is readily apparent. The motion approximately forms a 6x3 ellipse, which is to be expected, because the harmonic terms in the in-track direction are twice the harmonic terms in the radial direction. In addition, the position states are constrained to stay near the origin by the terminal condition that the spacecraft arrive at the origin after N steps. Figure 3 is a plot of required control energy versus sensor noise. The solid line shows the predicted fuel and the dots show the simulated fuel use requirements. The simulation results and the predicted values show close agreement. Having demonstrated the relevance of the prediction method, that method can be used to predict the effects of wide ranges of parameter variations.

A. MPC Parameter Identification

Model predictive controllers typically have a number of associated parameters that must be chosen. Among these are the prediction horizon length and the replan frequency. Figure 4 shows predictions of the effect of varying the horizon length and replan-frequency for a constant five meter square error box using the analytical prediction method. The velocity noise levels were bounded by $N_{\max} = 3$mm/s. In the lower-left quadrant of Figure 4, increasing the horizon length and lowering the replan frequency (increasing discretization time-step) both reduce the expected control cost. In the upper-right quadrant, increasing the plan length does not lower the expected fuel cost. There is a limit to how far the replan frequency can be lowered before the problem becomes infeasible. For fixed time-steps, there appears to be a critical plan length (indicated by a horizontal line) at approximately 0.3 orbits, above which the fuel costs are not significantly lowered by increasing the plan length. The critical plan length line roughly corresponds to the division (separating dark and light areas in Figure 4(b)) between

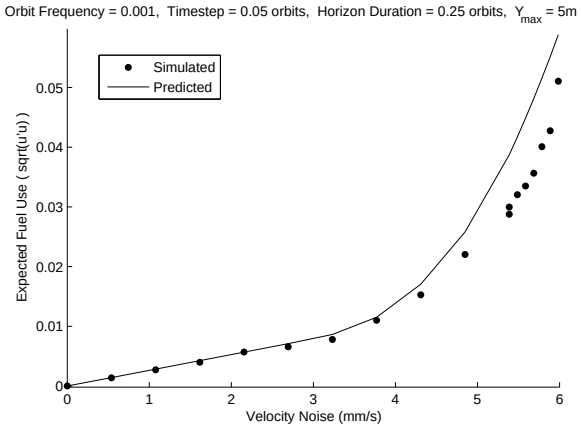

Fig.3: Comparison of Prediction Assumptions

the high- and low-disturbance regimes. Conceptually, the preferred planning horizon length is that at which the unconstrained LQR solution just begins to interact with the error box constraints. The vertical line indicates the replan rate that produces minimum fuel use. The prediction method indicates the most fuel-efficient combination of time-step and plan length lies at the intersection of the dashed lines in Figure 4.

By establishing how the effect of control parameters changes as the orbit period is altered, the prediction method can be used to aid the selection of both. Recreating the same contour plot for a different orbit ($n = 0.0005$) results in a graph (shown in Figure 5) with many of the same characteristics as the $n = 0.001$ graph. The preferred plan length (indicated by a horizontal line) has become slightly shorter, as has the preferred time-step.

B. Constraint Trades

The analytical prediction method enables the rapid optimization of control parameters for a variety of different trades relevant to planning a formation flying mission. CDGPS is a commonly examined method of sensing relative state and is known to produce estimates of velocity with sensing error between 0.5 mm/s and 2 mm/s [9]. Figure 6 shows contours of constant expected fuel use for the relation between error box size and noise level. Consider a scenario in which the noise is known to be 3 mm/s, slightly higher than a realistic GPS estimate. Setting the error box size to 1 meter gives an infeasible problem. If the error box size is increased to 3 meters, the problem becomes feasible. Further increases give a significant decrease in fuel use, up to a size of about 7 meters. This lies on the line of transition between constrained and unconstrained operation, beyond which there is no fuel-use gain for enlarging the error box. Therefore, like the choice of planning horizon, the ideal design is at the point where the constraints become active.

Another trade relevant to control system design is the relationship between error box size and planning horizon length. Figure 7 shows this trade for the example system. The fuel use numbers are low relative to those in the

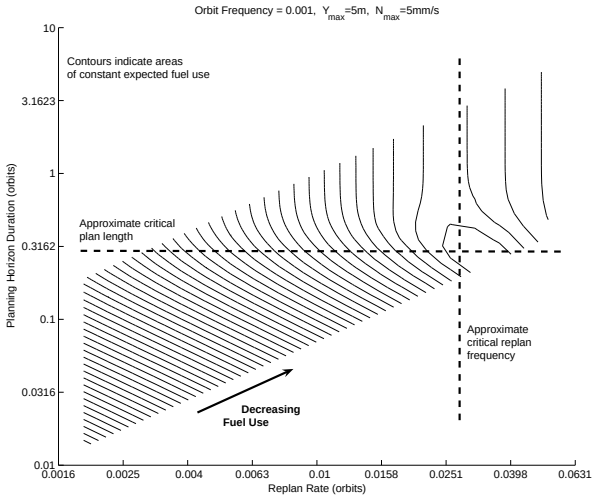

(a) Contours show fuel use decreases as prediction horizon is extended

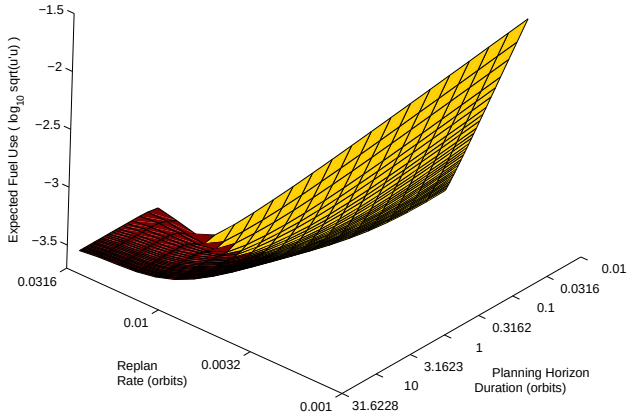

(b) Surface showing interaction between low and high noise regime models (note axes reversed from Fig. 4(a))

Fig.4: Effect of Plan Length and Replan Frequency on Fuel Use ($n = 0.001$)

literature [7], because the problem being examined has time-invariant linear dynamics and no process noise. The figure shows that fuel use is very high regardless of horizon length for error boxes smaller than ∼7 meters. For each error box larger than ∼7 meters, there is often a particular planning horizon length that gives the minimum expected fuel use. As in Figure 6, the expected fuel use is insensitive to error box size in many regions of the plot. For instance, when using a plan length of one orbit, the expected fuel use is the same for a 10 meter error box as for a 100 meter error box. This counterintuitive result is explained by the feasibility terminal constraint that requires the optimized trajectory to terminate at the origin. As a result, enlarging the error box beyond a certain size while holding the plan length constant does not reduce fuel use, because the spacecraft must still remain close to the origin.

IV. CONCLUSION

Results have been presented on the impact of noise on control for formation flying spacecraft. A form of MPC has